Control of High-Performance Mini- and Microscale *Electrical Cylinders*

Sergey Edward Lyshevski
Department of Electrical Engineering, Rochester Institute of Technology, Rochester, NY 14623-5603
E-mail: seleee@rit.edu, Web: www.rit.edu/~seleee

***Abstract* – The focus of this paper is the application of mini- and microscale *Electrical Cylinders* as high-performance translational actuators that guarantee fast and precise positioning. The objectives are to design, analyze, test and compare different control algorithms for closed-loop *Electrical Cylinders* with permanent-magnet direct current and synchronous servomotors. These *Electrical Cylinders* are widely used in aerospace, automotive, robotics and other electromechanical systems. For example, *Electrical Cylinders* displace the control surfaces of flight and undersea vehicles, robotic arms, etc. The major emphases are placed in the analysis and design of affordable, robust, efficient, and high torque density servos. *Electrical Cylinders* with different servomotors are tested in order to examine alternative solutions. The performance comparison is made for *Electrical Cylinders* regulated using distinct controllers. These control laws are designed and implemented using advanced DSPs, microcontrollers and VLSI controllers-drivers. We synthesize proportional-integral-derivative (PID), nonlinear, relay, and sliding mode controllers to guarantee the optimal (achievable) dynamic performance, stability, robustness, accuracy, etc. For different commands (angular or linear position and acceleration) and loads, accurate positioning and tracking with zero steady-state error are achieved. Our results illustrate that *Electrical Cylinders* with synchronous servomotors are the preferable solution in high-performance applications.**

I. Introduction

Overall electromechanical systems performance is significantly influenced by the actuator's power and torque densities, servomotor characteristics, kinematics, electronics, etc. To control these electromechanical systems, nonlinear control laws have been used. These controllers, implemented utilizing DSPs and microcontrollers, regulate advanced servomotors with attached mechanical structures. This paper highlights specific applications of the advanced actuators [1-3], power electronics, and control in order to demonstrate how high-performance mini- and microscale *Electrical Cylinders* should be designed, modeled, analyzed and implemented. We integrate hardware and software co-design to synthesize high-performance closed-loop systems.

To formulate and solve the motion control problem, coherent nonlinear models are used. Electromechanical transients of servomotors and dynamics of electronics are augmented. Applying the design procedures reported, nonlinear control algorithms are found. These controllers were implemented and tested. Through analytical and experimental results it is shown that the DSP- and VLSI controllers/ drivers-based closed-loop electromechanical systems guarantee robustness, stability, precise positioning, desired accuracy, required deflection rate, disturbance attenuation, and specified steady-state behavior.

The proof-of-concept demonstration test-beds are built in order to test different hardware solutions, control algorithms and software. It is demonstrated that by using the reported results, high-performance closed-loop *Electrical Cylinders* can be designed. The developed software enables one to perform nonlinear simulation, data-intensive analysis, optimization, and control execution algorithms. This software fully supports the advanced controllers designed. We have addressed and solved critical problems in the analysis and design of electromechanical systems for advanced applications

II. *Electrical Cylinders* and Actuator Technologies

Requirements, imposed on the electromechanical system performance, have generated a critical need for using advanced servos. To demonstrate the application of *Electrical Cylinders*, we consider the control surface actuators, see Figure 1. Servo-motors, integrated within the *Electrical Cylinder* kinematics, move control surfaces to attain the desired control features for underwater vehicles. These *Electrical Cylinder* can be equipped with hundreds of watts or milliwats servomotors. For example, the use of 500 W servomotor will allows one to achieve 25,000 N thrust with the linear velocity 2 m/sec, while micromotors will result in less than 1 N thrust. Different servomotors should be applied due to the specified rated and maximal torques required, velocity, acceleration, settling time, reliability, redundancy, etc. Rotational radial- and axial-topology MEMS-based high-speed miniservomotors with planetary gearheads have been fabricated and characterized [3]. For high-speed micro- and minimotors (volume within 1 cm^3), the torque and power densities can be as high as 2×10^{-3} N-m/cm^3 and 1 W/cm^3. The torque and power densities depend on permanent magnets, electromagnetic system, geometry, airgap, fabrication technologies, etc. The angular velocity of micromotors can be 100,000 rad/sec and higher. Planetary gears increase the torque and reduce the angular velocity.

Figure 1. *Electrical Cylinders*, MEMS-technology servomotor, and VLSI controller-driver

Advances in MEMS fabrication and novel electromagnetic topologies allow one to design and fabricate high-performance affordable electromagnetic servomotors with the outer diameter less that 1 mm. The matching electronics is available as high-performance system-on-a-chip VLSI controllers-drivers that, if needed, can be integrated with DSPs and microcontrollers. For miniscale electromechanical systems, there exist a wide variety of servomotors, sensors, power electronics, ICs and DSPs. This enables one to design efficient, high power/torque densities, reliable, robust, and affordable hardware. However, a spectrum of challenging problems remains in devising control algorithms using the optimized hardware solutions. In particular, there is a critical need to develop, verify, and implement advanced controllers to regulate servomotors with corresponding sensors and ICs. Complex ICs (MOSFET drivers, optocouplers, A/D and D/A converters, filters, output stages, Hall-effect circuitry, etc.) provide the interface between the DSPs, servomotors and sensors. This paper addresses the focused efforts on a number of thrust areas performing fundamental, applied, and experimental research. In particular, we

- develop high-performance affordable hardware solutions for MEMS/CMOS technology based *Electrical Cylinders*,
- perform modeling, simulation, analysis, optimization, and design based upon the hardware designed and deployed,
- design robust control algorithms,
- develop robust high-performance software,
- test and implement *Electrical Cylinders*.

Electrical Cylinders, actuated by high torque density servomotors, are studied to guarantee superior performance in terms of positioning accuracy, desired acceleration, minimum-time positioning, efficiency, stability, settling time, overshoot, robustness, reliability, tolerance, compactness, flexibility, ruggedness, simplicity, affordability, maintainability, etc. These closed-loop *Electrical Cylinders* integrate servomotors, resolvers and ICs, see Figures 2 and 3. The reference angular (or linear) displacement is assigned. Using reference and actual position (angular displacement is measured by the resolver and linear displacement can be sensed by different high-accuracy sensors), the controller develops the PWM signals to drive the high-frequency transistors of the output stage.

Different control algorithms can be implemented using advanced DSPs that guarantee a high degree of flexibility in the realization of control laws. The specialized Analog Devices and Texas Instruments DSPs also perform real-time analysis, diagnostics, filtering and decision-making. However, VLSI controllers-drivers (implement PID control algorithms) ensure robust cost-effective solution. For permanent-magnet servomotors, the voltages applied to the phase windings are controlled by changing the switching frequency or duty ratio. The rotor displacement of permanent-magnet synchronous motors is measured by the Hall-effect sensors to properly supply the phase voltages to the *as*, *bs* and *cs* stator windings guaranteeing the balance operation. These different hardware and software solutions require distinct control algorithms, and, in general, one cannot use *generic* controllers.

III. Modeling of Servos With DC Micromotors

Using the circuitry and *torsional-mechanical* dynamics of permanent-magnet DC motors, as well as the first-order VLSI controller-driver input-output dynamics, the following model is used to model the transient behavior

$$\begin{aligned}
\frac{du_a}{dt} &= -\frac{1}{T_{pa}}u_a + \frac{k_{pa}}{T_{pa}}d_D, \\
\frac{di_a}{dt} &= \frac{1}{L_a}u_a - \frac{r_a}{L_a}i_a - \frac{k_a}{L_a}\omega_r, \\
\frac{d\omega_r}{dt} &= \frac{k_a}{J}i_a - \frac{B_m}{J}\omega_r - \frac{1}{J}T_L, \\
\frac{d\theta_r}{dt} &= \omega_r,
\end{aligned} \tag{1}$$

with the rotational and translational output equations as

$\theta(t) = k_{kinematics}\theta_r(t)$ and $y(t) = k_{kinematics}\theta_r(t)$.

Here, u_a is the voltage applied to the motor armature winding (average ICs output voltage); i_a is the armature current; ω_r and θ_r are the rotor angular velocity and displacement; d_D is the duty ratio; T_L is the load torque; k_{pa} and T_{pa} are the coefficients of the VLSI controller-driver; r_a and L_a are the armature resistance and inductance; k_a is the *back emf* (*torque*) constant; B_m is the viscous friction coefficient; J is the equivalent moment of inertia.

From (1), one has the equation of motion in matrix form

$$\dot{x}(t) = Ax + Bu, \tag{2}$$

$$\begin{bmatrix} \frac{du_a}{dt} \\ \frac{di_a}{dt} \\ \frac{d\omega_r}{dt} \\ \frac{d\theta_r}{dt} \end{bmatrix} = \begin{bmatrix} -\frac{1}{T_{pa}} & 0 & 0 & 0 \\ \frac{1}{L_a} & -\frac{r_a}{L_a} & -\frac{k_a}{L_a} & 0 \\ 0 & \frac{k_a}{J} & -\frac{B_m}{J} & 0 \\ 0 & 0 & 1 & 0 \end{bmatrix} \begin{bmatrix} u_a \\ i_a \\ \omega_r \\ \theta_r \end{bmatrix} + \begin{bmatrix} \frac{k_{pa}}{T_{pa}} \\ 0 \\ 0 \\ 0 \end{bmatrix} d_D - \begin{bmatrix} 0 \\ 0 \\ \frac{1}{J} \\ 0 \end{bmatrix} T_L.$$

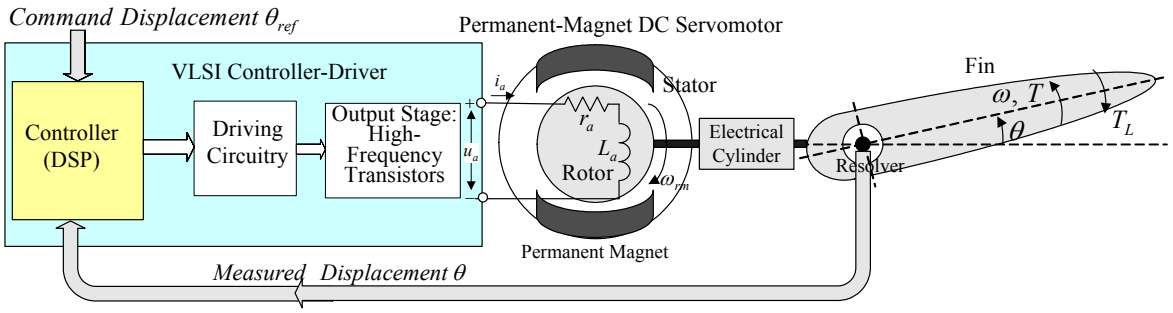

Figure 2. Closed-loop *Electrical Cylinder* (electromechanical system) with permanent-magnet DC servomotor

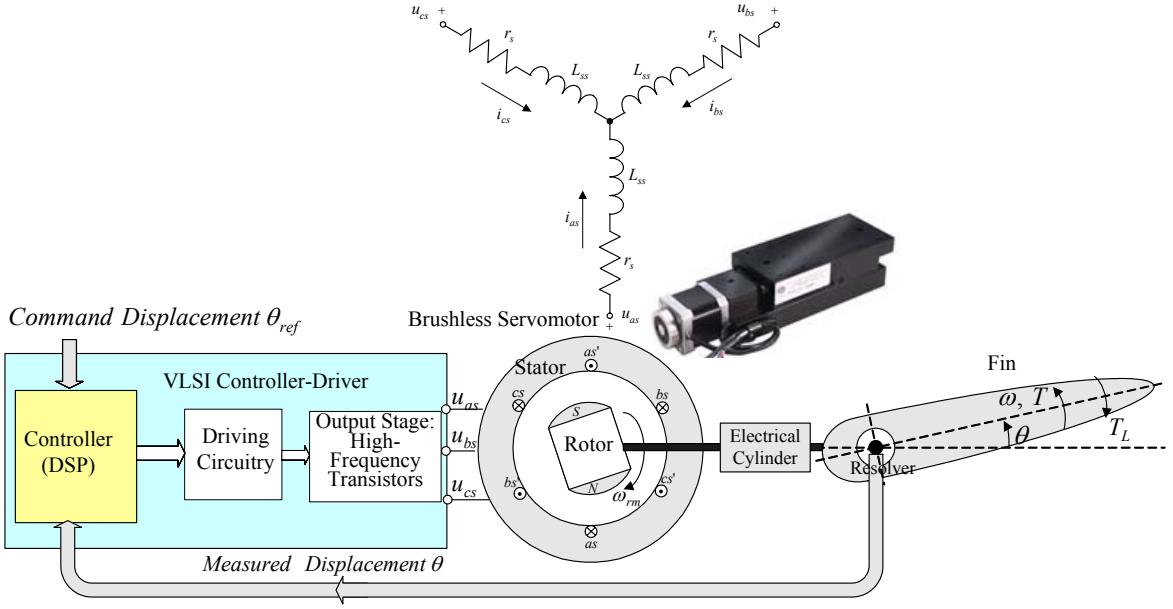

Figure 3. Closed-loop *Electrical Cylinder* with permanent-magnet synchronous servomotor

The angular displacement may be the output of the rotational electromechanical systems. That is,

$$\theta(t) = k_{kinematics}\theta_r(t),$$

where $k_{kinematics}$ is the kinematics coefficient which includes the *Electrical Cylinder* gear coefficient.

The linear displacement is the output if one examines the translational motions, and we have

$$y(t) = k_{kinematics}\theta_r(t).$$

IV. Control of Systems With DC Servomotors

4.1. Proportional-integral control

The positioning (tracking) error is the difference between the command and actual angular (or linear) displacements. That is, one obtains

$$e(t) = \theta_{ref}(t) - \theta(t) = \theta_{ref}(t) - k_{kinematics}\theta_r(t)$$

or

$$e(t) = y_{ref}(t) - y(t) = y_{ref}(t) - k_{kinematics}\theta_r(t).$$

The voltage, applied to the armature winding u_a (average PWM voltage from the VLSI controller-driver), is controlled by changing the FETs duty ratio. The duty ratio is bounded by ± 1, and, therefore $-1 \le d_D \le +1$.

The duty ratio is controlled by the DSP, microcontroller or digital/analog controller (embedded in the VLSI controller-driver). The bounded control laws must be designed and verified. The nonlinear proportional-integral (PI) controller is given as

$$u(t) = \text{sat}_{-1}^{+1}(e, \int e dt) = \text{sat}_{-1}^{+1}\left(\underbrace{\sum_{j=0}^{\varsigma} k_{pj} e^{\frac{2j+1}{2\beta+1}}}_{\text{proportion al}} + \underbrace{\sum_{j=0}^{\sigma} k_{ij} \int e^{\frac{2j+1}{2\mu+1}} dt}_{\text{integral}} \right), \quad (3)$$

where k_{pj} and k_{ij} are the proportional and integral feedback gains; ς, β, σ and μ are the nonnegative integers assigned by the designer to attain the specified criteria in stability and tracking accuracy.

Letting $\varsigma = \beta = \sigma = \mu = 0$, one obtains a bounded PI controller as given by $u(t) = \text{sat}_{-1}^{+1}\left(k_{p0}e(t) + k_{i0}\int e(t)dt\right)$.

4.2. Tracking integral and proportional-integral control

The tracking constrained integral control algorithm is designed by minimizing nonquadratic functional [5]

$$J = \int_{t_0}^{t_f} \left(\begin{bmatrix} x(t) \\ \int e(t)\,dt \end{bmatrix}^T Q \begin{bmatrix} x(t) \\ \int e(t)\,dt \end{bmatrix} + G \int \tan^{-1} u\,du \right) dt,$$

where Q and G are the weighting matrices.

The constrained integral controller is found as

$$u(t) = -\tanh\left(G^{-1} \begin{bmatrix} B \\ 0 \end{bmatrix}^T K \begin{bmatrix} x(t) \\ \int e(t)\,dt \end{bmatrix} \right), \quad -1 \le u \le 1.$$

The unknown matrix K is found by solving the nonlinear differential equations.

Therefore, we have the following bounded controller

$$d_D(t) = -\text{sat}_{-1}^{+1}\left(k_u u_a + k_i i_a + k_\omega \omega_r + k_\theta \theta_r + k_e \int e(t)dt \right).$$

In general, the integral controllers cannot guarantee the optimal performance. The tracking PI controllers can be derived utilizing the *state transformation* concept [5]. We introduce the z and v variables that are defined using the systems state and control variables as $z = \begin{bmatrix} x & u \end{bmatrix}^T$, $v = \dot{u}$.

For linear dynamic systems

$$\dot{z}(t) = \begin{bmatrix} A & B \\ 0 & 0 \end{bmatrix} z + \begin{bmatrix} 0 \\ I \end{bmatrix} v = A_z z + B_z v,\ y = H x^{sys},\ z(t_0) = z_0,$$

minimizing the quadratic performance functional $J = \int_{t_0}^{t_f} \left(z^T Q_z z + v^T G_z v \right) dt$, one finds the PI control law $u(t) = K_{F1} x(t) - K_{F1} x_0 + K_{F2} \int x(\tau)\,d\tau + u_0$ with state feedback because $x(t) = \begin{bmatrix} x^{sys}(t) & e(t) \end{bmatrix}^T$.

It should be emphasized that bounded (as was demonstrated) and relay (minimum-time) controllers can be designed minimizing the specific functionals. For example, by minimizing $J = \int_{t_0}^{t_f} \begin{bmatrix} x(t) \\ \int e(t)\,dt \end{bmatrix}^T Q \begin{bmatrix} x(t) \\ \int e(t)\,dt \end{bmatrix} dt$,

one obtains a relay control $u = -\text{sgn}\left(\begin{bmatrix} B \\ 0 \end{bmatrix}^T \dfrac{\partial V}{\partial \begin{bmatrix} x(t) \\ \int e(t)\,dt \end{bmatrix}} \right)$.

Correspondingly, we obtain

$$d_D(t) = -\text{sgn}\left(k_u u_a + k_i i_a + k_\omega \omega_r + k_\theta \theta_r + k_e \int e(t)dt \right).$$

These relay-type controller cannot be implemented in practice due to the chattering phenomenon. Therefore, relay-type control laws with dead zone are commonly used.

4.3. Sliding mode control

Hard- and soft-switching sliding mode control algorithms are synthesized in [4]. We apply the variable structure theory to design high-performance systems.

The smooth sliding manifold is given as

$$M = \left\{ (t,x,e) \in R_{\ge 0} \times X \times E \mid \upsilon(t,x,e) = 0 \right\}$$

$$= \bigcap_{j=1}^{m} \left\{ (t,x,e) \in R_{\ge 0} \times X \times E \mid \upsilon_j(t,x,e) = 0 \right\}.$$

The time-varying linear and nonlinear switching surfaces are

$$\upsilon(t,x,e) = \begin{bmatrix} K_{\upsilon x}(t) & K_{\upsilon e}(t) \end{bmatrix} \begin{bmatrix} x(t) \\ e(t) \end{bmatrix} = K_{\upsilon x}(t) x(t) + K_{\upsilon e}(t) e(t) = 0,$$

and $\upsilon(t,x,e) = K_{\upsilon x e}(t,x,e) = 0$.

The hard- and soft-switching mode controllers are

$$u(t,x,e) = -\text{sat}_{-1}^{+1}(\upsilon) \text{ and } u(t,x,e) = -\phi(\upsilon),$$

where ϕ is the nonlinear, bounded, continuous, differentiable one-to-one function, for example, tanh or erf [4].

The feedback gain coefficients are found using the conditions imposed on the Lyapunov pairs [4].

V. *Electrical Cylinder* Actuated by a DC Servomotor

We examine an *Electrical Cylinder* in the translational actuator application. The studied system is equipped with a miniscale MEMS-technology servomotor. Translational displacement of the load should be achieved within the assigned dynamic specifications. The complete hardware integrates sensors, ICs and microcontroller. Taking into the account the thrust and displacement, we use 5 V, 0.15 W, 6×10^{-4} N-m, 2000 rad/sec miniservomotor with a planetary gear. For this miniscale servomotor, the parameters are: $r_a(\cdot) \in [15_{T=20^oC}\ 21_{T=120^oC}]$ ohm, L_a = 0.001 H, $k_a(\cdot) \in [0.002_{T=20^oC}\ 0.0015_{T=120^oC}]$ V-sec/rad, $B_m = 2.7\times10^{-8}$ N-m-sec/rad and $J = 5\times10^{-7}$ kg-m^2.

For the VLSI controller-driver with the maximum output current 1 A, we have $k_{pa} = 10$ and $T_{pa} = 4\times10^{-5}$ sec.

The duty ratio is bounded, and $-1 \le d_D \le +1$. Our goal is to design and verify different control algorithms.

Using (3), the following bounded proportional-integral controller is designed and tested

$$d_D = \text{sat}_{-1}^{+1}\left(49e + 25 \int e dt \right).$$

The experimental analysis of the transient behavior is a very important task. Figure 4 depicts the displacement if the command (reference) displacement is 1 cm. For the cold minimotor, the settling time is 0.0043 sec (solid line). For the worst-case performance (if the motor temperature is 120°C), the overshoot for $y(t)$ is 14%, and the settling time is 0.008 sec, see Figure 4 (dashed line).

Our goal is to examine distinct control algorithms. Using the variable structure design concept, we synthesize the nonlinear switching surface as $k_1\theta_r + k_2 e + k_3 e^{\frac{1}{3}} = 0$. Using the Lyapunov stability theory, the feedback gains are found. A soft-switching sliding mode control law is

$$d_D = \tanh^{\frac{1}{3}}\left(-0.1\theta_r + 52e + 39e^{\frac{1}{3}} \right).$$

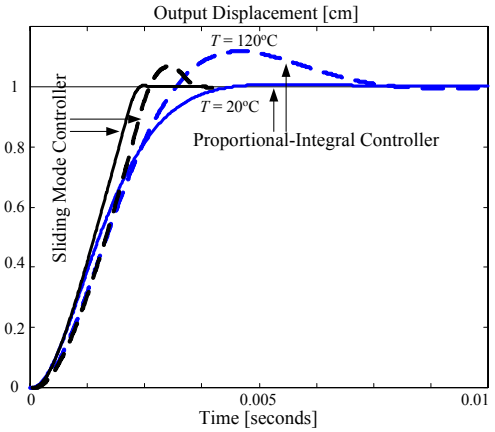

Figure 4. Dynamics with constrained PI and sliding mode control laws

Figure 4 documents the dynamics of the closed-loop minisystem with the sliding mode controller. The settling time is 0.0019 sec with no overshoot. For the worst-case performance (motor temperature is 120°C), the settling time is 0.0028 sec. The sliding mode controller guarantees faster dynamics, stability, robustness and fast acceleration compared with PI controllers. The results illustrate the efficiency of sliding mode controllers. However, from the implementation standpoints, it should be emphasized that one can implement PID-type control laws using VLSI controllers-drivers as a system-on-a-chip ICs solution. In contrast, DSPs or specialized application-specific VLSI controllers-drivers are needed to implement control algorithms with nonlinear feedback maps.

VI. Modeling of Electromechanical Systems With Permanent-Magnet Synchronous Motors

Two- and three-phase permanent-magnet synchronous micro- and minimotor guarantee superior performance. The schematic of *Electrical Cylinders* with three-phase synchronous servomotors is illustrated in Figure 5.

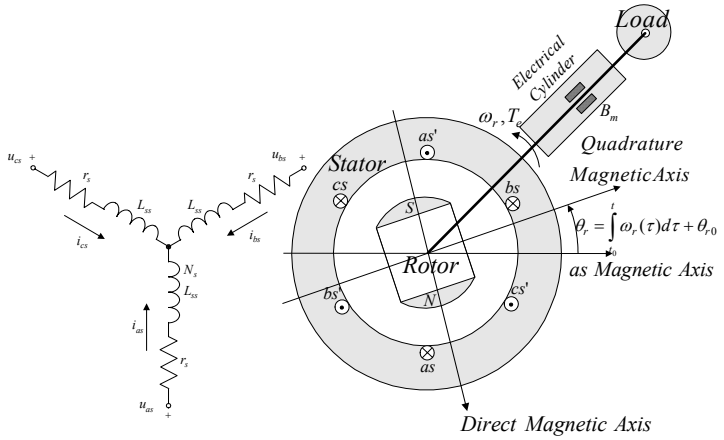

Figure 5. *Electrical Cylinders* with synchronous servomotor

Taking note of Kirchhoff's voltage law, the dynamics of the magnetically coupled *abc* stator windings is described by a set of differential equations

$$u_{as}=r_s i_{as}+\frac{d\psi_{as}}{dt},\ u_{bs}=r_s i_{bs}+\frac{d\psi_{bs}}{dt},\ u_{cs}=r_s i_{cs}+\frac{d\psi_{cs}}{dt},$$

where u_{as}, u_{bs} and u_{cs} are the applied phase voltages; i_{as}, i_{bs}, i_{cs} and ψ_{as}, ψ_{bs}, ψ_{cs} are the currents and flux linkages in the *abc* windings; r_s is the stator resistance.

Using the *quadrature-*, *direct-*, and *zero*-axis currents and voltages (i^r_{qs}, i^r_{ds}, i^r_{0s} and u^r_{qs}, u^r_{ds}, u^r_{0s}) and taking note of the Park transformation [6], one obtains a set of five differential equations

$$\frac{di^r_{qs}}{dt}=-\frac{r_s}{L_{ls}+\frac{3}{2}\overline{L}_m}i^r_{qs}-\frac{r_s}{L_{ls}+\frac{3}{2}\overline{L}_m}\omega_r-i^r_{ds}\omega_r+\frac{1}{L_{ls}+\frac{3}{2}\overline{L}_m}u^r_{qs},$$

$$\frac{di^r_{ds}}{dt}=-\frac{r_s}{L_{ls}+\frac{3}{2}\overline{L}_m}i^r_{ds}+i^r_{qs}\omega_r+\frac{1}{L_{ls}+\frac{3}{2}\overline{L}_m}u^r_{ds},$$

$$\frac{di^r_{0s}}{dt}=-\frac{r_s}{L_{ls}}i^r_{0s}+\frac{1}{L_{ls}}u^r_{0s},$$

$$\frac{d\omega_r}{dt}=\frac{3P^2\psi_m}{8J}i^r_{qs}-\frac{B_m}{J}\omega_r-\frac{P}{2J}T_L,\ T_e=\tfrac{3}{4}P\psi_m i^r_{qs},$$

$$\frac{d\theta_r}{dt}=\omega_r,$$

$$\theta=k_{kinematics}\theta_{rm}=\frac{2k_{kinematics}}{P}\theta_r,\ y=k_{kinematics}\theta_{rm}=\frac{2k_{kinematics}}{P}\theta_r,$$

where L_{ls} and $\overline{L}_m$ are the leakage and magnetizing inductances; ψ_m is the amplitude of the flux linkages established by the permanent magnets; P is the number of poles.

To regulate the angular position and acceleration, one changes the electromagnetic torque T_e. If the voltage-fed amplifiers are used, one changes the magnitude u_M of phase voltages regulating the duty ratio. A balanced voltage set is $u^r_{qs}=\sqrt{2}u_M$, $u^r_{ds}=0$ and $u^r_{0s}=0$.

VII. Control of *Electrical Cylinders* With Synchronous Servomotors

PID controllers that guarantee the balanced operation are:

- in the *machine* (*abc*) variables

$$u_{as}=\text{sat}^{+1}_{-1}\left(k_p e+k_i\int e dt+k_d\frac{de}{dt}\right)\cos\theta_r,$$

$$u_{bs}=\text{sat}^{+1}_{-1}\left(k_p e+k_i\int e dt+k_d\frac{de}{dt}\right)\cos\left(\theta_r-\tfrac{2}{3}\pi\right),$$

$$u_{cs}=\text{sat}^{+1}_{-1}\left(k_p e+k_i\int e dt+k_d\frac{de}{dt}\right)\cos\left(\theta_r+\tfrac{2}{3}\pi\right);$$

- in the *rotor* reference frame (*qd0* variables)

$$u^r_{qs}=\text{sat}^{+1}_{-1}\left(k_p e+k_i\int e dt+k_d\frac{de}{dt}\right),\ u^r_{ds}=0,\ u^r_{0s}=0.$$

In the *qd0* variables, applying the Lyapunov theory, the stability of the closed-loop system is proven using the quadratic function $V=\frac{1}{2}(i_{qs}^{r\ 2}+i_{ds}^{r\ 2}+\omega_r^2+\theta_r^2+e^2)$ [4]. One solves the Lyapunov inequality $\frac{dV(i_{qs}^r,i_{ds}^r,\omega_r,\theta_r,e)}{dt}<0$ to obtain the feedback gains.

Taking note of the ICs hardware, one changes the duty ratio, and six PWM outputs drive six transistors of the output stage. Digital and analog ICs (VLSI controllers-drivers) can be effectively used. By making use of the Hall-effect sensors, the logic circuitry is implemented to properly vary the high-frequency signals to switch *on* and *off* (*open* and *close*) high-frequency transistors in the four-quadrant power stage. The switching frequency varies from 1 to 10 MHz as a function of the rated voltage, current, and CMOS fabrication technology. The low-cost high-performance VLSI controllers-drivers are designed as a system-on-a-chip ICs (single ICs chip) and are straightforwardly used.

The proposed concept allows one to properly supply phase voltages to the phase windings to ensure the balanced operating conditions. It should be emphasized that if the *quadrature-direct* variables are used, the inverse Park transform is applied. Though the controller design is simple in the *qd0* reference frame, the real-time transformation to the *machine* variables must be performed by DSPs or using application-specific VLSI controllers-drivers.

VIII. *Electrical Cylinder* With a Synchronous Miniservomotor

We use a 4 mm permanent-magnet synchronous mini-servomotor with matching 4 mm planetary gearhead. This MEMS-technology surface micromachined 3 V, 8×10^{-4} N-m, 3000 rad/sec motor has the following parameters: $r_s(\cdot)\in[29_{T=20^oC}\ 40_{T=120^oC}]$ ohm, $L_{ss}=8\times10^{-5}$ H, $L_{ls}=1\times10^{-5}$ H, $\overline{L}_m=5\times10^{-5}$ H, $\psi_m(\cdot)\in[0.14_{T=20^oC}\ 0.1_{T=120^oC}]$ V-sec/rad or N-m/A, $B_m=3\times10^{-8}$ N-m-sec/rad and $J=5\times10^{-7}$ kg-m^2.

The following constrained PI control law is found and implemented using a VLSI controller-driver

$$d_D=\text{sat}_{-1}^{+1}\left(429e(t)+95\int e(t)dt\right).$$

This controller is verified through experiments. Different reference commands and loads were studied to analyze the transient dynamics, disturbance attenuation and accuracy. For the temperature range from 20°C to 120°C, r_s and ψ_m vary. This degrades the dynamics. Figure 6 illustrates the closed-loop miniservo behavior if $\begin{cases}1\,\text{cm}, & t\in[0\ \ 0.006]\,\text{sec}\\ 0.5\,\text{m}, & t\in(0.006\ \ 0.01]\,\text{sec}\end{cases}$. For 1 cm reference displacement, the settling times are 0.004 sec (solid line for $T=20^oC$) and 0.0042 sec (dashed line for $T=120^oC$) sec. For the hot servomotor, 3% overshoot is observed. Zero steady-state angular positioning error was achieved. We conclude that a high-performance closed-loop *Electrical Cylinder* system is designed.

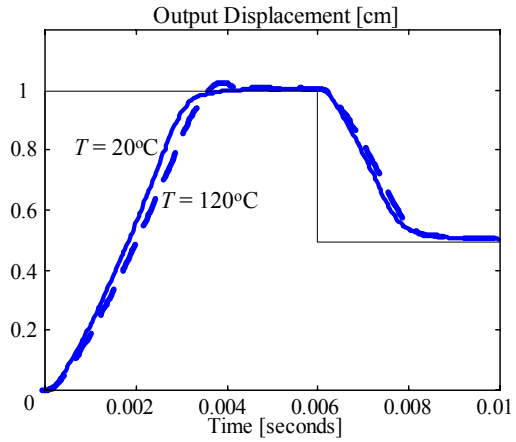

Figure 6. Experimental results: dynamics of the closed-loop system with a synchronous servomotor

IX. Conclusions

The advanced family of affordable integrated high-performance electromechanical systems with mini- and microscale *Electrical Cylinders* is needed to ultimately achieve the desired overall systems performances. We researched new emerging control methods applied to state-of-the-art high-performance hardware. The examined hardware solutions integrate servomotors, sensors, ICs, VLSI controllers-drivers, etc. Fundamental, applied and experimental results in design of electromechanical systems with permanent-magnet MEMS-technology servomotors are reported. Our particular interest was concentrated on the application of high torque density mini- and microscale actuators and ICs that have superior characteristics. It was found that permanent-magnet synchronous motors are very efficient, compact and rugged. In addition, they have higher torque density and efficiency compared with other servomotors. To solve a spectrum of problems in hardware and software developments, we found mathematical models, performed nonlinear simulations, analyzed and optimized servosystems, designed controllers, and solved software/hardware co-design problems. A number of important issues in control of closed-loop systems, implementation of high accuracy positioning sensors, application of DSP-based controllers, testing, and verification were studied. Precise positioning with zero steady-state error, stability and robustness were achieved.

References

1. P. L. Chapman and P. T. Krein, "Smaller is better? Prospectives on micromotors and electric drives," *IEEE Industry Applications Magazine*, no. 1, pp. 62-67, 2003.
2. M. K. Kurosawa, H. Itoh, K. Asai and T. Shigematsu, "Micro linear motor using surface acoustic wave device," *Proc. Symposium on Industrial Electronics*, vol. 2, pp. 383-387, 2002.
3. S. E. Lyshevski, *MEMS and NEMS: Systems, Devices, and Structures*, CRC Press, Boca Raton, FL, 2002.
4. S. E. Lyshevski, *Control Systems Theory With Engineering Applications*, Birkhäuser, Boston, MA, 2001.
5. S. E. Lyshevski, "Space transformation method in control of agile interceptors and missiles with advanced microelectromechanical actuators," *Proc. Conference on Decision and Control*, Maui, HI, 2003.
6. P. C. Krause, O. Wasynczuk and S. D. Sudhoff, *Analysis of Electric Machinery*. IEEE Press, New York, 1995.